Pt/CB-Catalyzed Chemoselective Hydrogenation Using in situ-Generated Hydrogen by Microwave Mediated Dehydrogenation of Methylcyclohexane under Continuous-Flow Conditions

Naoya Sakurada , Takanori Kitazono , Takashi Ikawa , Tsuyoshi Yamada * , Hironao Sajiki *

Posted Date: 24 May 2024

doi: 10.20944/preprints202405.1603.v1

Keywords: microwave-assisted organic synthesis; liquid organic chemical hydrides; heterogeneous catalyst; hydrogen production; chemoselective hydrogenation; platinum

 doi:10.20944/preprints202405.1603.v1

Article

Pt/CB-Catalyzed Chemoselective Hydrogenation Using *In Situ*-Generated Hydrogen by Microwave Mediated Dehydrogenation of Methylcyclohexane under Continuous-Flow Conditions

Naoya Sakurada, Takanori Kitazono, Takashi Ikawa, Tsuyoshi Yamada*, and Hironao Sajiki*

Laboratory of Organic Chemistry, Gifu Pharmaceutical University, 1-25-4 Daigaku-Nishi, Gifu 501-1196, Japan

* Correspondence: yamada@gifu-pu.ac.jp (T.Y.); sajiki@gifu-pu.ac.jp (H.S.)

Abstract: Hydrogen gas (H_2) has attracted attention as a next-generation clean energy source. Its efficient and safe preparation and utilization are crucial in both industry and organic chemistry. In this study, a Pt/CB-catalyzed MW-mediated continuous-flow hydrogenation reaction was developed using methylcyclohexane (MCH) as the reducing agent (hydrogen carrier). Alkynes, alkenes, nitro groups, benzyl esters, and aromatic chlorides were chemoselectively hydrogenated using Pt/CB under MW-assisted continuous-flow conditions. This methodology represents a safe and energy-efficient hydrogenation process, as it eliminates the need for an external hydrogen gas supply or heating jackets as a heat medium. Further application of MW-mediated continuous-flow hydrogenation reactions is a viable method for the efficient generation and utilization of sustainable energy.

Keywords: microwave-assisted organic synthesis; liquid organic chemical hydrides; heterogeneous catalyst; hydrogen production; chemoselective hydrogenation; platinum

1. Introduction

Hydrogen gas (H_2) is one of the most important and sustainable clean energy alternatives to fossil fuels because after the combustion of H_2, only H_2O is produced instead of greenhouse gases [1–3]. Owing to its usefulness and sustainability, H_2 is widely used as an energy source in fuel cells and holds promise for various applications as a carbon-free energy source [4–8]. H_2 also serves as a vital reducing agent in organic synthesis [9 and 10]. However, large-scale storage, transportation, and handling of molecular hydrogen are challenging, not only because of regulatory restrictions on highly flammable and explosive gases but also due to the need for control based on physical properties such as specific gravity, boiling point, and boil-off, as well as infrastructure development and other cost issues [11–18]. In response to these challenges, chemically stable substances known as liquid organic chemical hydrides (LOCH) have received much attention [13,19–24]. Methylcyclohexane (MCH) is a type of LOHC that can store more than 500 times its own volume of H_2 gas and can be transported via pipelines, tankers, and road tankers, which are part of the fossil fuel infrastructure [25–28]. Therefore, significant efforts have been devoted to the development of hydrogen extraction and utilization methods using MCH as a promising material for hydrogen storage applications [29–36]. Kobayashi et al. reported the continuous-flow hydrogenation reaction of olefins using H_2 gas extracted from MCH under a parallel catalyst cartridge system, which continuously generated H_2 gas from a heterogeneous Pt catalyst-packed cartridge, and a solution of a substrate possessing an olefin moiety flowed into another heterogeneous Pd catalyst-packed cartridge [37].

Microwave (MW)-assisted organic synthesis (MAOS) has attracted attention in terms of energy efficiency owing to the selective and rapid heating of target materials [38–40]. Platinum-group metal

 doi:10.20944/preprints202405.1603.v1

catalysts supported on powdered activated carbons, such as palladium on carbon (Pd/C) and platinum on carbon (Pt/C), exhibit a significant reaction enhancement effect because the activated carbons selectively absorb MW and are locally heated to form hot spots [41–44]. However, when Pd/C or Pt/C supported on powdered activated carbon with significantly high MW affinity was irradiated with MW, significant deactivation of the catalytic activity was observed due to superheating (e.g., sintering of platinum-group metals dispersed in activated carbon) accompanied by arc discharge [45,46]. To address this issue and maximize the use of the MW affinity of activated carbon for organic reactions, we applied bead-shaped activated carbon (CB; carbon beads) as a support for platinum-group metal catalysts in MW-mediated organic reactions under continuous-flow systems. Bead-shaped CB, having a large void space when packed, allows contact between each bead at a point, and the free electron transfer can be controlled, thus preventing overheating and maintaining the catalytic activity.

We developed a hydrogen extraction reaction from methylcyclohexane (MCH) [47] and 2-propanol (2-PrOH) [48] catalyzed by platinum-supported bead-shaped activated carbon (Pt/CB), which proceeded under single-mode MW irradiation conditions of only 10–20 W (Figure 1a). Furthermore, this MW-mediated selective CB heating reaction mechanism was developed into a Pt/CB-catalyzed intramolecular C–C bond formation reaction of diarylacetylene derivatives under MW-assisted continuous-flow conditions, namely, the synthesis of polycyclic aromatic compounds based on C–H activation [49] (Figure 1b). When an MCH solution of diphenylacetylene was pumped into a 5% Pt/CB packed catalyst cartridge irradiated at 10 W MW, intramolecular cyclization (C–C bond formation reaction) to produce phenanthrene was obtained as the main product, but at the same time, conventional contact hydrogenation of diphenyl ethane was also produced in a 40% yield. This reaction was reported after optimization studies, including changing the solvent to a mixture of MCH and 2-PrOH and tuning the reaction such that intramolecularly cyclized phenanthrene was highly selective [49] (Figure 1c). In this study, optimization studies focused on the continuous-flow alkyne hydrogenation reaction via MW, and a Pt/CB-catalyzed MW-mediated continuous-flow hydrogenation reaction with MCH as the reducing agent (hydrogen carrier) was developed (Figure 1d).

 doi:10.20944/preprints202405.1603.v1

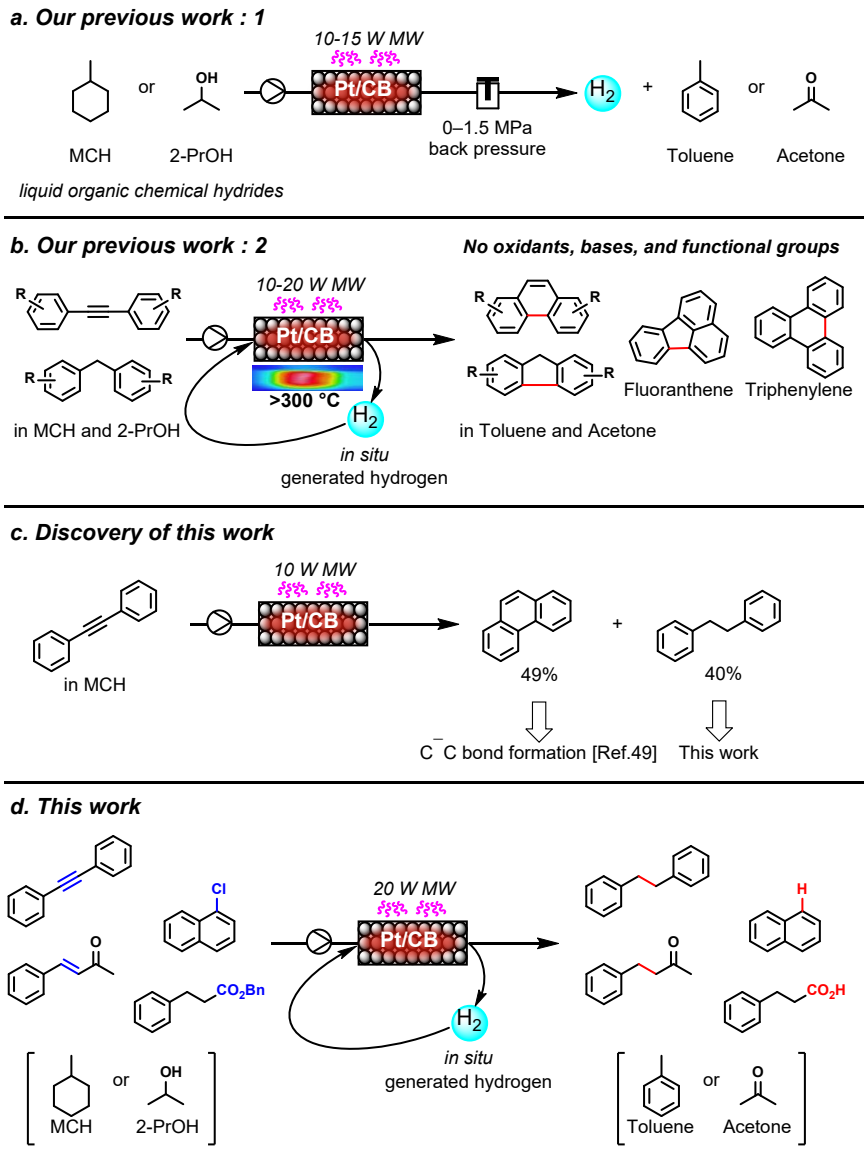

Figure 1. Background of the development of this research: a MW-mediated Pt/CB-catalyzed dehydrogenation reaction of LOCH. **b** MW-mediated Pt/CB-catalyzed selective aromatic cyclization reactions. **c** MW-mediated Pt/CB-catalyzed competitive reactions between aromatic cyclization and hydrogenation reactions. **d** MW-mediated Pt/CB-catalyzed selective hydrogenation reactions (this work).

2. Results and Discussion

2.1. Effect of Platinum-Group Metal Catalyts

For the initial investigation of the continuous-flow hydrogenation reaction using the MW-assisted dehydrogenation (hydrogen generation) reaction of MCH, the effect of the catalyst was explored using a single-mode MW flow apparatus (Table 1). A solution of benzalacetone (**1**, 0.25 mmol) in MCH (0.25 M) was introduced into an MW (max 20 W)-irradiated, catalyst (80 mg)-packed quartz cartridge at a flow rate of 0.25 mL/min at 140 °C. The 5% Pt/CB-catalyzed hydrogenation reaction efficiently produced hydrogenated 4-phenyl-2-butanone (**2**) in a ratio of 87%, with 13% of ethylbenzene (**4**) as the decomposed product due to overheating (Entry 1). When 1% Pt/CB was used, and the platinum metal content was reduced from 5% to 1%, platinum-catalyzed carbon-carbon bond cleavage reactions were apparently enhanced, with an increase in the percentage of 4 formed (43%) and a decrease in the percentage of the contact hydrogenation product 2 (57%, Entry 2). Palladium-

 doi:10.20944/preprints202405.1603.v1

and rhodium-supported carbon beads (Pd/CB and Rh/CB, respectively) exhibited low catalytic activity in the dehydrogenative aromatization of MCH under MW irradiation, with little hydrogen evolution and no progress in the catalytic hydrogenation reaction (Entries 3 and 4). Additionally, no hydrogenation activity was observed for CB without a metal (Entry 5).

Table 1. Effect of MW-mediated continuous-flow hydrogenation on CB-supported platinum-group metal species.

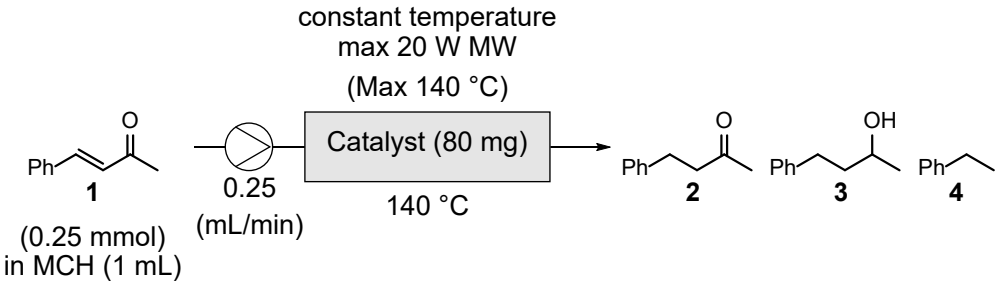

Entry	Catalyst	Product ratio[a] (1 : 2 : 3 : 4)
1	5% Pt/CB	0 : 87 : 0 : 13
2	1% Pt/CB	0 : 57 : 0 : 43
3	5% Pd/CB	94 : trace : 0 : 6
4	5% Rh/CB	95 : 0 : 0 : 5
5	CB	95 : 0 : 0 : 3

[a]The product ratio was determined by GC-FID using decane as an internal standard.

2.2. Effect of Temperature in the Catalyst Cartridge and Concentration of the Substrate Solution

First, the product ratios were investigated by mechanically controlling the MW strength and heating a catalyst cartridge filled with 5% Pt/CB at a constant temperature (120–150°C), while varying the substrate concentration in the pumped MCH (Table 2). An MCH (0.25 M) solution of **1** was introduced into a cartridge packed with 5% Pt/CB (80 mg) at a flow rate of 0.25 mL/min under MW irradiation. Compound **1** was completely consumed to yield **2** and **4** in a 72 : 28 ratio at 150 °C (Entry 1). As the temperature decreased from 150 to 140 °C, the ratio of **2** increased to 87% (Entry 2). The Pt/CB-catalyzed hydrogenation under MW irradiation (generation of **2**) became dominant over the decomposition-C bond cleavage reaction (generation of **4**) as the concentration was diluted from 0.25 to 0.05 M (Entry 3). In contrast, the ratio of **2** decreased at lower temperatures (130 °C and 120 °C) (Entries 4 and 5). It is reasonable to assume that the dehydrogenative aromatization reaction of MCH did not proceed sufficiently at 120 °C, resulting in insufficient hydrogen generation and insufficient activation of 5% Pt/CB.

Table 2. Effects of the reaction (cartridge) temperature and substrate concentration.

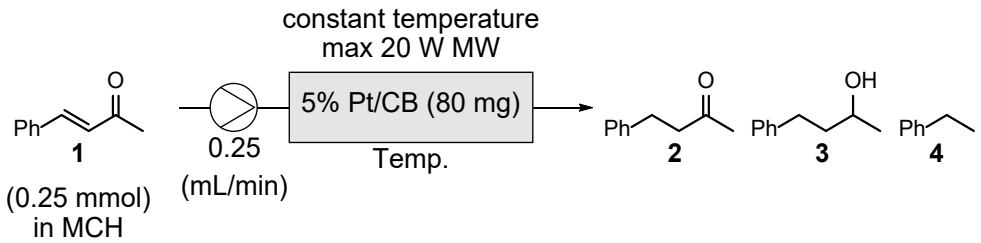

Entry	Temp. (°C)	Concentration (M)	Product ratio[a] (1 : 2 : 3 : 4)
1	150	0.25	0 : 72 : 0 : 28
2	140	0.25	0 : 87 : 0 : 13
3	140	0.05	0 : 92 : 0 : 8

 doi:10.20944/preprints202405.1603.v1

4	130	0.05	0 : 89 : 0 : 11
5	120	0.05	0 : 82 : 0 : 18

[a]The product ratio was determined by GC-FID using decane as the internal standard.

2.2. Effect of 2-PrOH as a Co-Solvent

Subsequently, the effect of the co-solvent was investigated (Table 3). We have previously demonstrated that C–C bond formation reactions proceed smoothly under MW irradiation using MCH with 2-PrOH as the co-solvent. Drawing from our earlier studies, various mixed solutions (0.05 M) of **1** were introduced into the 5% Pt/CB (80 mg)-packed quartz cartridge at 140 °C at a flow rate of 0.25 mL/min under MW (20 W) irradiation. When 2-PrOH was used as a co-solvent (MCH / 2-PrOH = 4 / 1), the ratio of **4** greatly decreased, and the ratio of **2** increased to 94%, but 5% of unreacted starting material (**1**) remained (Entry 2 vs. 1). When the proportion of 2-PrOH was reduced further to MCH / 2-PrOH = 19 / 1, 1 was completely consumed to yield **2** with a GC ratio of 98% and an isolated yield of 91% (Entry 3). The production ratio of **2** decreased slightly at a lower proportion of 2-PrOH (MCH / 2-PrOH = 99 / 1) (Entry 4). When only 2-PrOH was used as the flow solvent, the reaction efficiency significantly decreased (the production ratio of **2** was 48%), and 52% of **1** remained unchanged (Entry 5). The addition of an appropriate amount of 2-PrOH as a co-solvent improved the solubility of the substrate. Additionally, because 2-PrOH also absorbs MW, it was expected to dissipate the MW energy absorbed by 5% Pt/CB in the catalyst cartridge and suppress the thermally induced C–C cleavage reaction (generation of **4**). Thermographic measurements of the temperature of a quartz cartridge packed with 5% Pt/CB (80 mg) in an MW cavity (heater) mechanically set at 140 °C with the slit open showed that when an MCH solution of **1** (0.05 M) was pumped, the catalyst layer temperature reached 164 °C 30 minutes after the start of pumping. In contrast, the MCH / 2-PrOH = 19 / 1 solution of **1** (0.05 M) was 126 °C, which was lower than the set temperature. This result strongly supports the partial absorption effect of MW by 2-PrOH as a co-solvent disperses MW that would otherwise be absorbed by CB (Figure 2).

Table 3. Effect of 2-PrOH as a co-solvent.

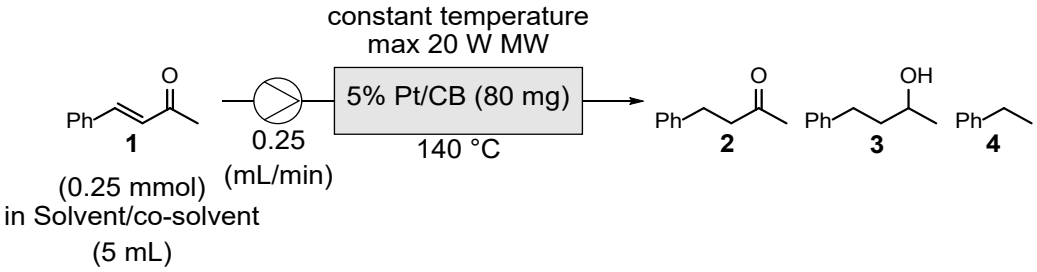

Entry	Solvent/co-solvent	Product ratio[a] (1 : 2 : 3 : 4)
1	MCH/-	0 : 92 : 0 : 8
2	MCH/2-PrOH = 4/1	5 : 94 : 0 : 1
3	MCH/2-PrOH = 19/1	0 : 98 (91)[b] : 0 : 2
4	MCH/2-PrOH = 99/1	0 : 95 : 0 : 5
5	2-PrOH/-	52 : 48 : 0 : trace

[a]The product ratio was determined by GC-FID using decane as the internal standard. [b]Isolated yield.

 doi:10.20944/preprints202405.1603.v1

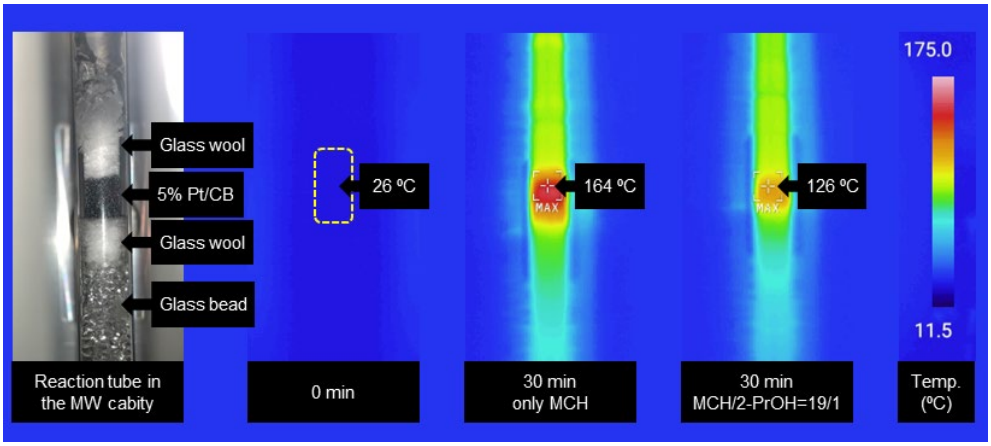

Figure 2. The surface temperature of a quartz cartridge packed with 5% Pt/CB (80 mg) in an MW cavity .

2.3. Scope of Applicable Substrates

The substrate applicability and chemoselectivity of MW-assisted hydrogenation reactions were also investigated (Table 4). Each substrate (0.0125–0.05 M, flow rate: 0.25 mL/min) dissolved in a mixed solvent of MCH and 2-PrOH (19:1) was flowed through a 5% Pt/CB (80 mg) packed catalyst cartridge at a mechanically controlled temperature of 140 °C.

Catalytic hydrogenation of alkenes (**1**) and alkyne (**5**) proceeded continuously, producing the corresponding alkanes (**2** and **6**), respectively (Entries 1 and 2). The 5% Pt/CB effectively catalyzed the hydrogenolysis of benzyl ester (CO_2Bn, **8**) to yield the carboxylic acid derivative (**9**) (Entry 3), but did not affect the aliphatic benzyl ether (**10**) under these conditions (Entry 4). The aromatic nitro group of compound **12** was selectively hydrogenated to an amine (**13**) at 165 °C (Entry 5), while increasing the reaction temperature to 190 °C resulted in naphthalene (**14**) as a single product (Entry 6), which underwent hydrogenolysis of the nitro group's C–N bond. Aliphatic and aromatic ketones (**1** and **15**) were stable under hydrogenation conditions with the 5% Pt/CB catalyst (Entries 1 and 7). The hydrogenative dechlorination of compound **17** proceeded smoothly at 190 °C without deactivation of 5% Pt/CB, and without neutralization of the hydrogen chloride formed during the reaction, resulting in the quantitative production of compound **14** (Entry 8).

Table 4. Scope of applicable substrates[a.]

Preprints.org (www.preprints.org) | NOT PEER-REVIEWED | Posted: 24 May 2024 doi:10.20944/preprints202405.1603.v1

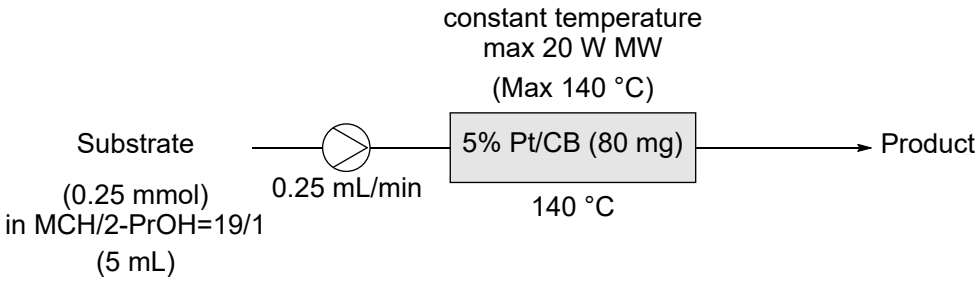

Entry	Substrate	Product	Ratio[b]	Yield (%)[c]
1	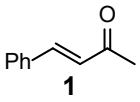 **1**	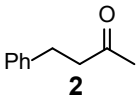 **2**	0 : 100	91
2[d,e]	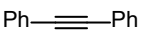 **5**	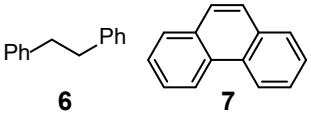 **6** **7**	0 : 97 : 3	95
3[f]	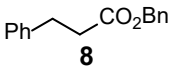 **8**	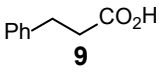 **9**	0 : 100	80
4	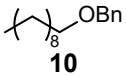 **10**	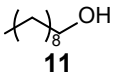 **11**	100 : 0	0 (88)[g]
5[h]	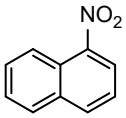 **12**	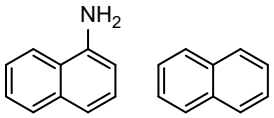 **13** **14**	19 : 72 : 9	68
6[i]			0 : 0 : 100	80
7	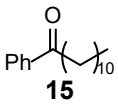 **15**	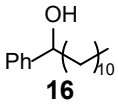 **16**	100 : 0	0 (91)[g]
8[i]	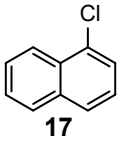 **17**	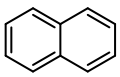 **14**	0 : 100	87

[a]A solution of the substrate (0.25 mmol) in MCH/2-PrOH (0.05 M, 0.25 mL min^{-1}) was pumped into the cartridge packed with 5% Pt/CB (80 mg) under MW irradiation conditions keeping the temperature constant at 140 °C. [b]The ratio of substrate to product was determined using ^{1}H NMR spectroscopy. [c]Isolated yields. [d]The concentration of the substrate solution was 0.0125 M. [e]MCH was used as a solvent in the absence of 2-PrOH. [f]The concentration of the substrate solution was 0.025 M. [g]The recovered yield of substrate. [h]The temperature of the catalyst cartridge was 165 °C. [h]The temperature of the catalyst cartridge was 190 °C.

3. Materials and Methods

3.1. Materials

All reagents and solvents were obtained from commercial sources and used without further purification. ^{1}H NMR and ^{13}C NMR spectra were recorded on JEOL JNM ECA-500 (500 MHz for ^{1}H NMR and 125 MHz for ^{13}C NMR) and ECZ-400 (400 MHz for ^{1}H NMR and 100 MHz for ^{13}C NMR) spectrometers. $CDCl_3$ was used as the solvent for NMR measurements. The chemical shifts (δ) are expressed in parts per million and internally referenced (0.00 ppm for tetramethylsilane and 77.0 ppm

 doi:10.20944/preprints202405.1603.v1

for $CDCl_3$ in ^{13}C NMR). The continuous-flow microwave reactor (EYELA, MR-2G-100) was developed by Tokyo Rikakikai Co., Ltd. (Tokyo, Japan); see product URL: https://eyela.actibookone.com/content/detail?param=eyJjb250ZW50TnVtIjoyMTY4MX0=&detailFlg=1&pNo=44. The quartz tube used as the catalyst cartridge was purchased from Tokyo Rikakikai Co., Ltd. An FMR-100 (Saida FDS Inc., Shizuoka, Japan) was used to flow the reaction solution. Thermo FLEX F50 was used as a thermal imaging camera for monitoring the temperature of a quartz cartridge. Catalysts such as 5% Pt/CB, 5% Pd/CB, 5% Rh/CB, and CB were obtained from N.E. CHEMCAT Co. (Tokyo, Japan). The ^1H NMR spectra of known products are identical to those reported in the literature.

3.2. General Procedure for Hydrogenations (Table 4)

The flow path was equipped with a 5% Pt/CB (80.0 mg) packed EYELA reaction tube and flowed with a mixed solvent of MCH and 2-PrOH at a flow rate of 0.25 mL/min at 140 °C under a maximum of 10 W MW irradiation for 5 min. The substrate in the mixed solvent (0.05 M) was then pumped into the reaction tube under the same conditions, and the flow path was rinsed four times with the mixed solvents (1 mL × 3, then 20 mL × 1) using the pump. MW irradiation was stopped, and a mixed solvent of ethyl acetate/toluene (1/1, 40 mL) was pumped to further wash the entire flow path. The entire reaction mixture and wash solution were collected and concentrated *in vacuo*, dissolved in $CDCl_3$, and analyzed by ^1H NMR spectroscopy using 1,1,2,2-tetrachloroethane (52.5 μL, 0.5 mmol) as an internal standard. If necessary, the product was further purified using silica gel column chromatography (hexane / EtOAc).

3.3. Spectroscopic Data of Products

4-Phenyl-2-butanone (Table 4 Entry 1) [CAS Reg. No. 2550-26-7]. Obtained in 91% yield (33.7 mg, 228 μmol; colorless solid) from 4-phenyl-3-buten-2-one (34.5 mg, 250 μmol). ^1H NMR [400 MHz (ECZ-400, $CDCl_3$)] δ 7.31–7.26 (m, 2H), 7.22–7.18 (m, 3H), 2.90 (t, J = 7.6 Hz, 2H), 2.77 (t, J = 7.6 Hz, 2H), 2.15 (s, 3H); ^{13}C NMR [100 MHz (ECZ-400, $CDCl_3$)] δ 208.0, 140.9, 128.5, 128.3, 126.1, 45.2, 30.1, 29.7. The ^1H NMR spectra were identical to those reported previously [50].

1,2-Diphenylethane (Table 4 Entry 2) [CAS Reg. No. 103-29-7]. Obtained in 95% yield (43.0 mg, 236 μmol; colorless solid) from diphenylacetylene (44.6 mg, 250 μmol). ^1H NMR [400 MHz (ECZ-400, $CDCl_3$)] δ 7.31–7.27 (m, 4H), 7.22–7.18 (m, 6H), 2.92 (s, 4H); ^{13}C NMR [100 MHz (ECZ-400, $CDCl_3$)] δ 141.7, 128.4, 128.3, 125.9, 37.9. The ^1H NMR spectra were identical to those reported previously [51].

3-Phenylpropionic acid (Table 4 Entry 3) [CAS Reg. No. 501-52-0]. Obtained in 76% yield (30.1 mg, 201 μmol; colorless solid) from benzyl 3-phenylpropionate (60.1 mg, 250 μmol). ^1H NMR [400 MHz (ECZ-400, $CDCl_3$)] δ 7.32–7.29 (m, 2H), 7.23–7.21 (m, 3H), 2.97 (t, J = 7.8 Hz, 2H), 2.69 (t, J = 7.8 Hz, 2H); ^{13}C NMR [100 MHz (ECZ-400, $CDCl_3$)] δ 179.2, 140.1, 128.5, 128.2, 126.4, 35.6, 30.5. The ^1H NMR spectra were identical to those reported previously [51].

Benzyl decyl ether (Table 4 Entry 4) [CAS Reg. No. 87220-50-6]. Recovered in 88% yield (54.7 mg, 220 μmol; colorless liquid). ^1H NMR [400 MHz (ECZ-400, $CDCl_3$)] δ 7.37–7.28 (m, 5H), 4.50 (s, 2H), 3.46 (t, J = 6.6 Hz, 2H), 1.65–1.58 (m, 2H), 1.37–1.26 (m, 14H), 0.88 (t, J = 6.9 Hz, 3H); ^{13}C NMR [100 MHz (ECZ-400, $CDCl_3$)] δ 138.7, 128.3, 127.6, 127.4, 72.8, 70.5, 31.9, 29.7, 29.6, 29.6, 29.5, 29.3, 26.2, 22.7, 14.1. The ^1H NMR spectra were identical to those reported previously [52].

1-Amino naphthalene (Table 4 Entry 5) [CAS Reg. No. 134-32-7]. Obtained in 68% yield (24.3 mg, 170 μmol; red solid) from 4-nitronaphthalene (43.3 mg, 250 μmol). ^1H NMR [400 MHz (ECZ-400, $CDCl_3$)] δ 7.81–7.72 (m, 2H), 7.45–7.37 (m, 2H), 7.31–7.24 (m, 2H), 6.72 (dd, J = 7.1, 1.6 Hz, 1H), 3.95 (brs, 2H); ^{13}C NMR [100 MHz (ECZ-400, $CDCl_3$)] δ 142.0, 134.3, 128.5, 126.3, 125.8, 124.8, 123.5, 120.7, 118.8, 109.6. The ^1H NMR spectra were identical to those reported previously [53].

Naphthalene (Table 4 Entry 6 and 8) [CAS Reg. No. 91-20-3]. Obtained in 80% yield (25.6 mg, 200 μmol; colorless solid) from 4-nitronaphthalene (43.3 mg, 250 μmol). Obtained in 89% yield (28.5 mg, 223 μmol; colorless solid) from 4-chloronaphthalene (40.7 mg, 250 μmol). ^1H NMR [400 MHz (ECZ-400, $CDCl_3$)] δ 7.87–7.83 (m, 4H), 7.50–7.46 (m, 4H); ^{13}C NMR [100 MHz (ECZ-400, $CDCl_3$)] δ 133.4, 127.9, 125.8. The ^1H NMR spectra were identical to those reported previously [54].

 doi:10.20944/preprints202405.1603.v1

1-Dodecaphenone (Table 4 Entry 7) [CAS Reg. No. 1674-38-0]. Recovered in 91% yield (59.3 mg, 228 μmol; colorless solid). ^{1}H NMR [400 MHz (ECZ-400, $CDCl_3$)] δ 7.98–7.95 (m, 2H), 7.56 (t, J = 7.2 Hz, 1H), 7.46 (t, J = 7.4 Hz, 2H), 2.96 (t, J = 7.5 Hz, 2H), 1.77-1.70 (m, 2H), 1.39–1.26 (m, 16H), 0.88 (t, J = 6.9 Hz, 3H); ^{13}C NMR [100 MHz (ECZ-400, $CDCl_3$)] δ 200.6, 137.0, 132.8, 128.5, 128.0, 38.6, 31.9, 29.6, 29.5, 29.5, 29.4, 29.3, 24.3, 22.7, 14.1. The ^{1}H NMR spectra were identical to those reported previously [55].

4. Conclusions

We achieved the direct transfer of hydrogen from methylcyclohexane (MCH) to reducible functional groups by means of microwave (MW)-assisted dehydrogenation. Compared to conventional continuous-flow hydrogenations, which typically rely on externally supplied combustible hydrogen gas, this safer method uses MCH both as a hydrogen carrier and as a flow solvent. It efficiently utilizes in situ dehydrogenation reactions supported by low-dose single-frequency MW irradiation and Pt(0) supported on carbon beads. Reducible functionalities such as alkynes, alkenes, nitro groups, benzyl esters, and aromatic chlorides were chemoselectively hydrogenated by a Pt/CB-catalyzed MW-mediated continuous-flow hydrogenation reaction. In contrast, 5% Pt/CB showed no catalytic activity for the hydrogenation of aliphatic benzyl ethers, and aromatic and aliphatic ketones. Within the flow reaction cartridge, 5% Pt/CB created a local high-temperature reaction field, and the reaction proceeded efficiently because the CB selectively absorbed MW energy. The MW energy required for this reaction was only 10–20 W. The practical implementation of this reaction is expected to contribute to the use of hydrogen as a sustainable energy source and advance synthetic organic chemistry.

Supplementary Materials: The following supporting information can be downloaded from: www.mdpi.com/xxx/s1, Figure S1: The microwave flow reactor (EYELA, MR-2G-100); Figure S2: The quartz tube for the continuous flow microwave reactor (EYELA, MR-2G-100); Content 1: General; Content 2: MW flow device (EYELA), catalyst cartridge, and peripheral devices; Content 3: Thermographic measurements of the temperature of a 5% Pt/CB-packed cartridge (Figure 2); Content 4: Spectral data of products; Content 5: References; Content 6: ^{1}H and ^{13}C spectra of products.

Author Contributions: Writing—original draft and supporting information preparation: N.S., T.K., and T.Y.; designing the research: N.S., T.I., T.Y., and H.S.; investigation, experiment, and analysis: N.S., T.K., T.I., and T.Y.; project administration, supervision, funding acquisition, and writing—review and editing: H.S. All authors have read and agreed to the published version of the manuscript.

Funding: This study was partially funded by a Grant-in-Aid from the Japan Society for the Promotion of Science (JSPS) KAKENHI (Grant Number 20H03367) for H.S., a project commissioned by the New Energy and Industrial Technology Development Organization (NEDO, Project code: P19004), and a Sasakawa Scientific Research Grant from the Japan Science Society for N.S.

Data Availability Statement: The **Supplementary Materials** are available free of charge on the website.

Acknowledgments: This work was partially supported by the JST Support for Pioneering Research Initiated by the Next Generation (SPRING) Program (Number JPMJSP2142). We thank Tokyo Rikakikai Co., Ltd., and SAIDA FDS Inc. for lending the MW flow devices and providing constructive suggestions. We also thank N.E. CHEMCAT Co. for providing heterogeneous platinum-group metal catalysts and Editage (www.editage.jp) for English editing.

Conflicts of Interest: The authors declare no conflicts of interest.

References

1. Armaroli, N.; Balzani, V. The Hydrogen Issue. *ChemSusChem* **2011**, *4*, 21–36. https://doi.org/10.1002/cssc.201000182
2. Megía, P.J.; Vizcaíno, A.J.; Calles, J.A.; Carrero, A. Hydrogen Production Technologies: From Fossil Fuels toward Renewable Sources. A Mini Review. *Energy Fuels* **2021**, *35*, 16403–16415. https://doi.org/10.1021/acs.energyfuels.1c02501
3. Kumar, R.; Singh, R.; Dutta, S. Review and Outlook of Hydrogen Production through Catalytic Processes. *Energy Fuels* 2024, 38, 4, 2601–2629. https://doi.org/10.1021/acs.energyfuels.3c04026

4. Wang, Z.; Yang, Y.; Zhao, Z.; Zhang, P.; Zhang, Y.; Liu, J.; Ma, S.; Cheng, P.; Chen, Y.; Zhang, Z. Green synthesis of olefin-linked covalent organic frameworks for hydrogen fuel cell applications. *Nat. Commun.* **2021**, *12*, 1982. https://doi.org/10.1038/s41467-021-22288-9
5. Jiao, K.; Xuan, J.; Du, Q.; Bao, Z.; Xie, B.; Wang, B.; Zhao, Y.; Fan, L.; Wang, H.; Hou, Z.; Huo, S.; Brandan, N.P.; Yin, Y.; Guiver, M. D. Designing the next generation of proton-exchange membrane fuel cells. *Nature* **2021**, *595*, 361–369. https://doi.org/10.1038/s41586-021-03482-7
6. Allendorf, M.D.; Stavila, V.; Snider, J.L.; Witman, M.; Bowden, M.E.; Brooks, K.; Tran, B.L.; Autrey, T. Challenges to developing materials for the transport and storage of hydrogen. *Nat. Chem.* **2022**, *14*, 1214–1223. https://doi.org/10.1038/s41557-022-01056-2
7. Chen, L.; Song, Z.; Zhang, S.; Chang, C.; Chuang, Y.; Peng, X.; Dun, C.; Urban, J.J.; Guo, J.; Chen, J.; Prendergast, D.; Salmeron, M.; Somorjai, G.A.; Su, J. Ternary NiMo-Bi liquid alloy catalyst for efficient hydrogen production from methane pyrolysis. *Science* **2023**, *381*, 857–861. 10.1126/science.adh8872
8. Liu, R.; He, G.; Wang, X.; Mallapragada, D.; Zhao, H.; Shao-Horn, Y.; Jiang, B. A cross-scale framework for evaluating flexibility values of battery and fuel cell electric vehicles. *Nat. Commun.* **2024**, *15*, 280. https://doi.org/10.1038/s41467-023-43884-x
9. Irrgang, T.; Kempe, R. Transition-Metal-Catalyzed Reductive Amination Employing Hydrogen. *Chem. Rev.* **2020**, *120*, 9583–9674.
10. Nishimura, S. *Handbook of Heterogeneous Catalytic Hydrogenation for Organic Synthesis*; John Wiley and Sons, Inc.: Hoboken, NJ, USA, 2001; pp. 1–38.
11. Rivard, E.; Trudeau, M.; Zaghib, K. Hydrogen Storage for Mobility. A Review. *Materials* **2019**, *12*, 1973. https://doi.org/10.3390/ma12121973
12. Aziz, M. Liquid Hydrogen: A Review on Liquefaction, Storage, Transportation, and Safety. *Energies* **2021**, *14*, 5917. https://doi.org/10.3390/en14185917
13. Song, S.; Lin, H.; Sherman, P.; Yang, X.; Nielsen, C.P.; Chen, X.; McElroy, M.B. Production of hydrogen from offshore wind in China and cost-competitive supply to Japan. *Nat. Commun.* **2021**, *12*, 6953. https://doi.org/10.1038/s41467-021-27214-7
14. Hodges, A.; Hoang, A.L.; Tsekouras, G.; Wagner, K.; Lee, C.; Swiegers, G.F.; Wallace, G.G. A high-performance capillary-fed electrolysis cell promises more cost-competitive renewable hydrogen. *Nat. Commun.* **2022**, *13*, 1304. https://doi.org/10.1038/s41467-022-28953-x
15. Al Ghafri, S.Z.; Munro, S.; Cardella, U.; Funke, T.; Notardonato, W.; Trusler, J.M.; Leachman, J.; Span, R.; Kamiya, S.; Pearce, G. Hydrogen liquefaction: A review of the fundamental physics, engineering practice and future opportunities. *Energy Environ. Sci.* **2022**, *15*, 2690–2731. https://doi.org/10.1039/d2ee00099g
16. Kang, D.; Yun, S.; Kim, B.-k. Review of the Liquid Hydrogen Storage Tank and Insulation System for the High-Power Locomotive. *Energies* **2022**, *15*, 4357. https://doi.org/10.3390/en15124357
17. Guo, J.; Zhang, Y.; Zavabeti, A.; Chen, K.; Guo, Y.; Hu, G.; Fan, X.; Li, G.K.; Hydrogen production from the air. *Nat. Commun.* **2022**, *13*, 5046. https://doi.org/10.1038/s41467-022-32652-y
18. Ghorbani, B.; Zendehboudi, S.; Saady, N.M.C.; Duan, X.; Albayati, T.M. Strategies To Improve the Performance of Hydrogen Storage Systems by Liquefaction Methods: A Comprehensive Review. *ACS Omega* **2023**, *8*, 18358–18399. https://doi.org/10.1021/acsomega.3c01072
19. Niermann, M.; Drünert, S.; Kaltschmitt, M.; Bonhoff, K. Liquid organic hydrogen carriers (LOHCs) – techno-economic analysis of LOHCs in a defined process chain. *Energy Environ. Sci.* **2019**, *12*, 290–307. https://doi.org/10.1039/c8ee02700e
20. Oh, J.; Bathula, H.B.; Park, J.H.; Suh, Y. A sustainable mesoporous palladium-alumina catalyst for efficient hydrogen release from N-heterocyclic liquid organic hydrogen carriers. *Commun. Chem.* **2019**, *2*, 68. https://doi.org/10.1038/s42004-019-0167-7
21. Wang, C.; Astruc, D. Recent developments of nanocatalyzed liquid-phase hydrogen generation. *Chem. Soc. Rev.* **2021**, *50*, 3437. https://doi.org/10.1039/d0cs00515k
22. Cho, J.-Y.; Kim, H.; Oh, J.-E.; Park, B.Y. Recent Advances in Homogeneous/Heterogeneous Catalytic Hydrogenation and Dehydrogenation for Potential Liquid Organic Hydrogen Carrier (LOHC) Systems. *Catalysts* **2021**, *11*, 1497. https://doi.org/10.3390/catal11121497
23. Yu, H.; Li, X.; Zheng, J. Beyond Hydrogen Storage: Metal Hydrides for Catalysis. *ACS Catal.* **2024**, *14*, 3139–3157. https://doi.org/10.1021/acscatal.3c05696
24. Rampai, M. M.; Mtshali, C.B.; Seroka, N.S.; Khotseng, L. Hydrogen production, storage, and transportation: recent advances. *RSC Adv.* **2024**,*14*, 6699–6718. https://doi.org/10.1039/D3RA08305E
25. Obara, S. Energy and exergy flows of a hydrogen supply chain with truck transportation of ammonia or methyl cyclohexane. *Energy* **2019**, *174*, 848–860. https://doi.org/10.1016/j.energy.2019.01.103
26. Modisha, P.M.; Ouma, C.N.M.; Garidzirai, R.; Wasserscheid, P.; Bessarabov, D. The Prospect of Hydrogen Storage Using Liquid Organic Hydrogen Carriers. *Energy Fuels* **2019**, *33*, 2778–2796. https://doi.org/10.1021/acs.energyfuels.9b00296

27. Wijayanta, A.T.; Oda, T.; Purnomo, C.W.; Kashiwagi, T.; Azizb, M. Liquid hydrogen, methylcyclohexane, and ammonia as potential hydrogen storage: Comparison review. *Int. J. Hydrogen Energy* **2019**, *44*, 15026–15044. https://doi.org/10.1016/j.ijhydene.2019.04.112
28. Rao, P.C.; Yoon, M. Potential Liquid-Organic Hydrogen Carrier (LOHC) Systems: A Review on Recent Progress. *Energies* **2020**, *13*, 6040. https://doi.org/10.3390/en13226040
29. Al-ShaikhAli, A.H.; Jedidi, A.; Anjum, D.H.; Cavallo, L.; Takanabe, K. Kinetics on NiZn Bimetallic Catalysts for Hydrogen Evolution via Selective Dehydrogenation of Methylcyclohexane to Toluene. *ACS Catalysis* **2017**, *7*, 1592–1600. https://doi.org/10.1021/acscatal.6b03299
30. Takise, K.; Sato, A.; Ogo, S.; Seo, J.G.; I, K.; Kado, S.; Sekine, Y. Low-temperature selective catalytic dehydrogenation of methylcyclohexane by surface protonics. *RSC Adv.* **2019**, *9*, 27743–27748. https://doi.org/10.1039/C9RA06042A
31. Hamayun, M.H.; Maafa, I.M.; Hussain, M.; Aslam, R. Simulation Study to Investigate the Effects of Operational Conditions on Methylcyclohexane Dehydrogenation for Hydrogen Production. *Energies* **2020**, *13*, 206. https://doi.org/10.3390/en13010206
32. Zhang, X.; He, N.; Lin, L.; Zhu, Q.; Wang, G.; Guo, H. Study of the carbon cycle of a hydrogen supply system over a supported Pt catalyst: Methylcyclohexane–toluene–hydrogen cycle. *Catal. Sci. Technol.* **2020**, *10*, 1171–1181. https://doi.org/10.1039/C9CY01999E
33. Kojima, H.; Matsuda, T.; Kano, K.; Tsujimura, T. Methylcyclohexane production under fluctuating hydrogen flow rate conditions. *Int. J. Hydrogen Energy* **2021**, *46*, 9433–9442. https://doi.org/10.1016/j.ijhydene.2020.12.117
34. Meng, J.; Zhou, F.; Ma, H.; Yuan, X.; Wang, Y.; Zhang, J. A Review of Catalysts for Methylcyclohexane Dehydrogenation. *Top Catal.* **2021**, *64*, 509–520. https://doi.org/10.1007/s11244-021-01465-6
35. Ye, H.L.; Liu, S.X.; Zhang, C.; Cai, Y.Q.; Shi, Y.F. Dehydrogenation of methylcyclohexane over Pt-based catalysts supported on functional granular activated carbon. *RSC Adv.* **2021**, *11*, 29287–29297. https://doi.org/10.1039/D1RA05480E
36. Chen, L.; Verma, P.; Hou, K.; Qi, Z.; Zhang, S.; Liu, Y.; Guo, J.; Stavila, V.; Allendorf, M.D.; Zheng, L.; Salmeron, M.; Prendergast, D.; Somorjai, G.A.; Su, J. Reversible dehydrogenation and rehydrogenation of cyclohexane and methylcyclohexane by single-site platinum catalyst. *Nat. Commun.* **2022**, *13*, 1092. https://doi.org/10.1038/s41467-022-28607-y
37. Miyamura, H.; Suzuki, A.; Zhu, Z.; Kobayashi, S. Hydrogen Generation from Organic Hydrides under Continuous-Flow Conditions Using Polymethylphenylsilane-Aluminum Immobilized Platinum Catalyst. *Chem. Asian J.* **2022**, *17*, e202200569. https://doi.org/10.1002/asia.202200569
38. Kappe, C. O. Controlled microwave heating in modern organic synthesis. *Angew. Chem. Int. Ed.* **2004**, *43*, 6250–6284. https://doi.org/10.1002/anie.200400655
39. Kappe, C. O. Microwave dielectric heating in synthetic organic chemistry. *Chem. Soc. Rev.* **2008**, *37*, 1127–1139. https://doi.org/10.1039/B803001B
40. Gao, Y.; Remón, J.; Matharu, A. S. Microwave-assisted hydrothermal treatments for biomass valorization: a critical review. *Green Chem.* **2021**, *23*, 3502–3525. https://doi.org/10.1039/d1gc00623a
41. Horikoshi S.; Osawa A.; Sakamoto S.; Serpone N. Control of microwave-generated hot spots. Part V. Mechanisms of hot-spot generation and aggregation of catalyst in a microwave-assisted reaction in toluene catalyzed by Pd-loaded AC particulates. *Applied Catalysis A: General*. **2013**, *460–461*, 52–60. https://doi.org/10.1016/j.apcata.2013.04.022
42. Horikoshi, S.; Kamata, M.; Mitani, T.; Serpone, N. Control of microwave-generated hot spots. 6. Generation of hot spots in dispersed catalyst particulates and factors that affect catalyzed organic syntheses in heterogeneous media. *Ind. Eng. Chem. Res.* **2014**, *53*, 14941–14947. https://doi.org/10.1021/ie502169z
43. Días-Ortiz, Á.; Prieto, P.; de la Hoz, A. A critical overview on the effect of microwave irradiation in organic synthesis. *Chem. Rec.* **2019**, *19*, 85–97. https://doi.org/10.1002/tcr.201800059
44. Ahmad, A.A.; Al-Raggad, M.; Shareef, N. Production of activated carbon derived from agricultural by-products via microwave-induced chemical activation: a review. *Carbon Lett.* **2021**, *31*, 957–971. https://doi.org/10.1007/s42823-020-00208-z
45. Chen, W.; Gutmann, B.; Kappe, C. O. Characterization of microwave-induced electric discharge phenomena in metal–solvent mixtures. *ChemistryOpen* **2012**, *1*, 39–48. https://doi.org/10.1002/open.201100013
46. Horikoshi, S.; Arai, Y.; Ahmad, I.; DeCamillis, C.; Hicks, K.; Schauer, B.; Serpone, N. Application of Variable Frequency Microwaves in Microwave-Assisted Chemistry: Relevance and Suppression of Arc Discharges on Conductive Catalysts. *Catalysts* **2020**, *10*, 777. https://doi.org/10.3390/catal10070777
47. Ichikawa,T.; Matsuo, T.; Tachikawa, T.; Yamada, T.; Yoshimura, T.; Yoshimura, M.; Takagi, Y.; Sawama, Y.; Sugiyama, J.; Monguchi, Y.; Sajiki, H. Microwave-Mediated Site-Selective Heating of Spherical-Carbon-Bead-Supported Platinum for the Continuous, Efficient Catalytic Dehydrogenative Aromatization of Saturated Cyclic Hydrocarbons. *ACS Sustainable Chem. Eng.* **2019**, 7, 3052–3061. https://doi.org/10.1021/acssuschemeng.8b04655

 doi:10.20944/preprints202405.1603.v1

48. Ichikawa, T.; Matsuo, T.; Tachikawa, T.; Teranishi, W.; Yamada, T.; Sawama, Y.; Monguchi, Y.; Sajiki, H. Microwave-Mediated Continuous Hydrogen Abstraction Reaction from 2-PrOH Catalyzed by Platinum on Carbon Bead. *Catalysts* **2019**, *9*, 655. https://doi.org/10.3390/catal9080655
49. Yamada, T.; Teranishi, W.; Sakurada, N.; Otri, S.; Abe, Y.; Matsuo, T.; Morii, Y.; Yoshimura, M.; Yoshimura, T.; Ikawa, T.; Sajiki, H. Microwave-assisted C–C bond formation of diarylacetylenes and aromatic hydrocarbons on carbon beads under continuous-flow conditions. *Commun. Chem.* **2023**, *6*, 78. https://doi.org/10.1038/s42004-023-00880-y
50. Colbon, P.; Ruan, J.; Purdie, M.; Mulholland, K.; Xiao, J. Double Arylation of Allyl Alcohol via a One-Pot Heck Arylation–Isomerization–Acylation Cascade. *Org. Lett.* **2011**, *13*, 5456–5459. https://doi.org/10.1021/ol202144z
51. Monguchi, Y.; Ida, T.; Maejima, T.; Yanase, T.; Sawama, Y.; Sasai, Y.; Kondo, S.; Sajiki, S. Palladium on Carbon-Catalyzed Gentle and Quantitative Combustion of Hydrogen at Room Temperature. *Adv. Synth. Catal* **2014**, *356*, 313–318. https://doi.org/10.1002/adsc.201300710
52. Gao, Y.; Yang, C.; Bai, S.; Liu, X.; Wu, Q.; Wang, J.; Jiang, C.; Qi, X. Visible-Light-Induced Nickel-Catalyzed Cross-Coupling with Alkylzirconocenes from Unactivated Alkenes. *Chem* **2020**. *6*, 675–688. https://doi.org/10.1016/j.chempr.2019.12.010
53. Yue, H.; Guo, L.; Liu, X.; Rueping, M. Nickel-Catalyzed Synthesis of Primary Aryl and Heteroaryl Amines via C–O Bond Cleavage. *Org. Lett.* **2017**, *19*, 1788–1791. https://doi.org/10.1021/acs.orglett.7b00556
54. Yamada, T.; Ogawa, A.; Masuda, H.; Teranishi, W.; Fujii, A.; Park, K.; Ashikari, Y.; Tomiyasu, N.; Ichikawa, T.; Miyamoto, R.; Bai, H.; Matsuyama, K.; Nagaki, A.; Sajiki, H. Pd catalysts supported on dual-pore monolithic silica beads for chemoselective hydrogenation under batch and flow reaction conditions. *Catal. Sci. Technol*. **2020**, *10*, 6359–6367. https://doi.org/10.1039/D0CY01442G
55. Hu, P.; Tan, M.; Cheng, L.; Zhao, H.; Feng, R.; Gu, W.; Han, W. Bio-inspired iron-catalyzed oxidation of alkylarenes enables late-stage oxidation of complex methylarenes to arylaldehydes. *Nat. Commun.* **2019**, *10*, 2425. https://doi.org/10.1038/s41467-019-10414-7